Impact Loads for Structural Damage Identification

Andrzej Swiercz, Jan Holnicki-Szulc, Przemyslaw Kolakowski

7th European Workshop on Structural Health Monitoring
July 8-11, 2014. La Cité, Nantes, France

IMPACT LOADS FOR STRUCTURAL DAMAGE IDENTIFICATION

Andrzej Świercz[1], **Jan Holnicki-Szulc**[1], **Przemysław Kołakowski**[2]

[1] *Institute of Fundamental Technological Research, Polish Academy of Sciences, Pawińskiego 5B, 02-106 Warsaw, Poland*
[2] *Adaptronica R&D company, Szpitalna 32, 05-092 Łomianki, Poland*

andrzej.swiercz@ippt.pan.pl

ABSTRACT

In this paper we numerically study simple two dimensional frame structure loaded by impulse-like excitations. Various configurations of time duration of a single impact load and location of this excitation are investigated. The aim of this research is to indicate the best possible load case for identification of a specific damage. Two kinds of structural modifications are considered. The first group concerns the element stiffness changes (axial and bending) which can be simulated by alternating the Young's modulus. The second group covers the modifications of stiffness nodal connections. In a numerical model, these kinds of defects can be implemented using rotational spring with different characteristics. Obtained selected responses for the original and modified structure are numerically generated.

KEYWORDS : *structural modification, semi-rigid joint, virtual distortion method, gradient-based optimization.*

INTRODUCTION

The damage identification problem is formulated as an optimization task exploiting the responses computed for the original and modified structure. The structural modifications are modeled using the Virtual Distortion Method (VDM) efficiently combined with the Finite Element Method (FEM). A modification of a finite element is modeled by imposing an initial deformation on that element – the so-called *virtual distortion*. The pre-stressed state of the structure is obtained by imposing an initial deformation on that element, without external loading. The formula for updated responses is a superposition of the original (with external load only) and pre-stressed state. The VDM technique allows for analytical gradient computation which can be successfully used in the gradient-based optimization problems.

The VDM technique is a versatile, fast reanalysis tool [1]. It has been used for identification of stiffness or mass modifications in trusses and frames when subjected to dynamic [2] or harmonic [3, 4] excitations. The application of this method is also suitable for various types of engineering analyses including optimal remodeling [5, 6], progressive collapse [7], adaptive impact absorption [8,9], detection of leakages in water distribution networks [10], detection of delamination in composite structures [11], identification of defects in electrical circuits [12].

1. DESIGN VARIABLES AND OPTIMIZATION PROCEDURE

In this paper we deal with Euler-Bernoulli beam structures under a determined load. Structural modifications (the design variables) to be identified at first are parametrized using the so-called *virtual distortions* and next optimized utilizing the selected dynamic responses obtained for the original and modified structure. Two types of modifications are considered. The first of them concerns the stiffness connection of an element with a node (semi-rigid joint) whereas the second is based on the modification of an element stiffness (longitudinal and bending).

1.1 Parametrization of the semi-rigid joints

A semi-rigid nodal connection of a beam can be modelled by a linear rotational spring. The torsional moment M_α acting on the spring is equal to the bending moment at the adjacent end of the beam and generates the angle of rotation $\overset{0}{\varphi}_\alpha$ in the spring and in the beam. Thus, the constitutive law of the spring can be expressed in terms of the nodal curvature κ_α and the angle of rotation $\overset{0}{\varphi}_\alpha$. For two characteristics *a.* and *b.* presented in Figure 1(a), the above mentioned relations can be written in the following forms:

$$\kappa_\alpha = \overset{0}{\varphi}_{\underline{\alpha}} \tan \psi_{\underline{\alpha}} = \overset{0}{\varphi}_{\underline{\alpha}} s_{\underline{\alpha}} \qquad \text{for} \qquad 0 \le \mu_\alpha \le \frac{1}{2} \qquad \text{and} \qquad \psi_\alpha = \frac{\pi}{2}\mu_\alpha^{\mathrm{n}}, \tag{1}$$

$$\overset{0}{\varphi}_\alpha = \kappa_{\underline{\alpha}} \tan \Theta_{\underline{\alpha}} = \kappa_{\underline{\alpha}} p_{\underline{\alpha}} \qquad \text{for} \qquad \frac{1}{2} < \mu_\alpha \le 1 \qquad \text{and} \qquad \Theta_\alpha = \frac{\pi}{2}(1-\mu_\alpha^{\mathrm{n}}), \tag{2}$$

where $s_\alpha = \tan\psi_\alpha$ is the rotational stiffness (cf. Figure 1(b)) and $p_\alpha = \tan\theta_\alpha$ is the rotational compliance (cf. Figure 1(c)) of the spring. The dimensionless nodal stiffness parameter $\mu_\alpha^{\mathrm{n}} \in \langle 0,1\rangle$ can be expressed by ψ_α or θ_α, which are valid in the range $\langle 0, \frac{\pi}{2}\rangle$. However, for avoiding singularities during computations limitations are assumed for $\psi \in \langle 0, \frac{\pi}{4}\rangle$ and for $\theta \in \langle 0, \frac{\pi}{4}\rangle$. In Equations (1) and

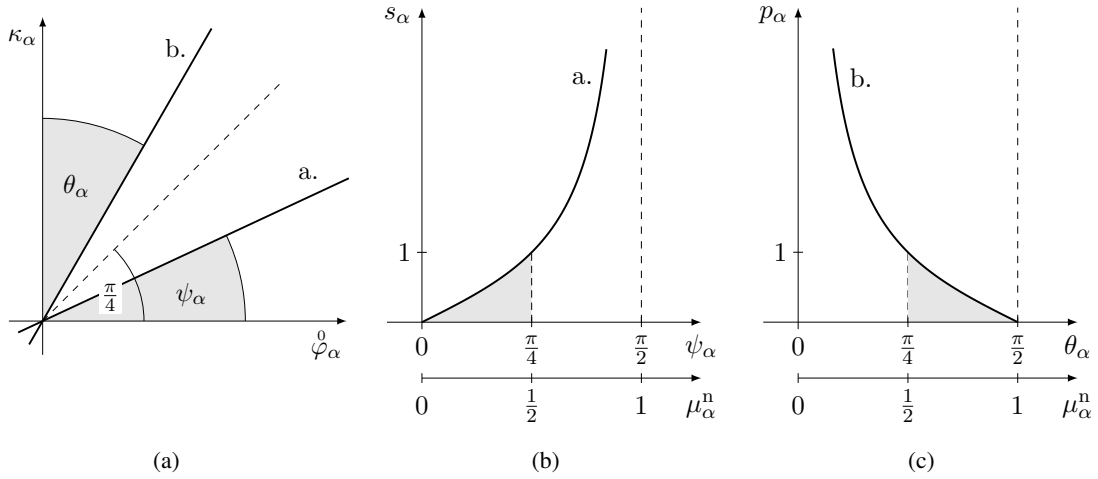

(a) (b) (c)

Figure 1 : (a) Curvature-angle of rotation characteristics for a linear rotational spring. (b) Graph of the connection stiffness as a function of parameter μ_α^{n}. (c) Graph of the connection compliance as a function of parameter μ_α^{n}.

(2) the angle of rotation $\overset{0}{\varphi}_\alpha$ is named the angular virtual distortion and is equivalent to the curvature virtual distortion by the relation $\overset{0}{\kappa}_\alpha = \frac{4}{l_{\underline{\alpha}}}\overset{0}{\varphi}_{\underline{\alpha}}$ at modelled connection of the beam with the length l_α. The updated nodal curvatures κ_α of the structure with the imposed curvature virtual distortions $\overset{0}{\kappa}_\alpha$ can be expressed using the VDM technique as follows:

$$\kappa_\alpha(t) = \overset{\mathrm{L}}{\kappa}_\alpha(t) + \sum_{\tau=0}^{t} B_{\alpha\beta}(t-\tau)\,\overset{0}{\kappa}_\beta(\tau) - \overset{0}{\kappa}_\alpha(t), \tag{3}$$

where $\overset{\mathrm{L}}{\kappa}_\alpha$ are the nodal curvatures of the original structure and $B_{\alpha\beta}(t)$ is the time-dependent curvature influence matrix containing nodal curvatures obtained by imposing the unit curvature virtual distortions (i.e. $\overset{0}{\kappa}_\alpha = 1$) at modelled nodal connections of the structure. Substitution of Equation (3) into Equations (1) and (2) leads to the relationship for determining the virtual distortions $\overset{0}{\kappa}_\alpha$ for given stiffness modification parameter μ_α^{n}. The resulting equation has to be solved for each time step t.

Analogously to the Equation (3), arbitrarily selected structural responses (e.g. nodal displacements, accelerations) can be updated knowing the curvature virtual distortions $\overset{0}{\kappa}_\alpha$ using the following formula:

$$f_i^{\mathrm{n}}(t) = \overset{\mathrm{L}}{f}_i^{\mathrm{n}}(t) + \sum_{\tau=0}^{t} \hat{B}_{i\alpha}(t-\tau)\,\overset{0}{\kappa}_\alpha(\tau), \tag{4}$$

where $\overset{\mathrm{L}}{f}_i(t)$ is the response of the intact structure and $\hat{B}_{i\alpha}(t)$ is the generalised influence matrix containing selected responses computed for the unit virtual distortions. More detailed description for modelling of the semi-rigid joints can be found in [13].

1.2 Parametrization of the stiffness of beams

Let us define the vector of element stiffness modifications $\mu_\alpha^{\mathrm{e}} = \frac{\hat{k}_\alpha}{k_\alpha}$, where k_α and $\hat{k}_\alpha$ are stiffness parameters of an intact and modified structure. In order to simplify, we assume modification of the Young's modulus, which leads to $\mu_\alpha^{\mathrm{e}} = \frac{\hat{E}_\alpha}{E_\alpha}$. The modifications can be modelled by the strain virtual distortions $\overset{0}{\varepsilon}_\alpha$ imposed on the elements of the original structure. We postulate that the structure modelled by the virtual distortions and the modified structure are identical in the sense of generalized strains and stresses at each time step t, which leads to the relationship:

$$\mu_{\underline{\alpha}}^{\mathrm{e}}\,\varepsilon_{\underline{\alpha}}(t) = \varepsilon_\alpha(t) - \overset{0}{\varepsilon}_\alpha(t), \tag{5}$$

where ε_α is a strain component for the beam element. Two dimensional beam element has three basic strain components and Equation (5) has to be fulfilled for each of them (see [3]). Analogously, there are three components of the virtual distortions $\overset{0}{\varepsilon}_\alpha$ corresponding to the strain components ε_α. On the other hand, the updated strain $\varepsilon_\alpha(t)$ can be computed using the VDM-technique:

$$\varepsilon_\alpha(t) = \overset{\mathrm{L}}{\varepsilon}_\alpha(t) + \sum_{\tau=0}^{t} D_{\alpha\beta}(t-\tau)\,\overset{0}{\varepsilon}_\beta(\tau), \tag{6}$$

where $D_{\alpha\beta}(t)$ is the strain influence matrix, whose columns contain strain obtained by consecutively imposing the unit strain virtual distortions $\overset{0}{\varepsilon}_\alpha(0) = 1$ on the modelled elements at the first time step of computations. By solving the set of Equations (5) and (6), the virtual distortions $\overset{0}{\varepsilon}_\alpha(t)$ are determined. Analogously to the Equation (4), the virtual distortions $\overset{0}{\varepsilon}_\alpha(t)$ can be used for updating the generalized response:

$$f_i^{\mathrm{e}}(t) = \overset{\mathrm{L}}{f}_i^{\mathrm{e}}(t) + \sum_{\tau=0}^{t} \hat{D}_{i\alpha}(t-\tau)\,\overset{0}{\varepsilon}_\alpha(\tau), \tag{7}$$

where $\hat{D}_{\alpha\beta}(t)$ is the pre-computed generalized influence matrix whose columns contain the generalized response calculated for the unit strain virtual distortions imposed on the modelled elements.

The in-depth discussion for modelling of the stiffness parameters for the beam element (longitudinal and bending) including cross-section area and formulation in the frequency domain is presented in [14].

1.3 Optimization procedure

The identification of the design parameter μ_α (i.e. μ_α^{n} or μ_α^{e}) can be formulated as a gradient-based optimization problem utilizing responses obtained for the original and the modified structure. At each iteration virtual distortions ($\overset{0}{\kappa}_\alpha$ or $\overset{0}{\varepsilon}_\alpha$) are determined which allow for efficient updating the

modelled response $f_i(\mu_\alpha,t)$. The applied optimization procedure leads to matching the modelled response $f_i(\mu_\alpha,t)$ to the response $f_i^M(\mu_\alpha,t)$ obtained for the modified structure as closely as possible. The following objective function is proposed:

$$F(\mu_\alpha)=\sum_i \frac{\sum_t \left(f_i(\mu_\alpha,t)-f_i^M(t)\right)^2}{\sum_t \left(f_i^M(t)\right)^2}. \tag{8}$$

The vector μ_α can be iteratively determined using e.g. the steepest descent method (SD):

$$\mu_\alpha^{k+1}=\mu_\alpha^k-\Delta F^k\frac{F_{,\alpha}}{||F_{,\alpha}||^2}, \tag{9}$$

where the upper superscript $k+1$ denotes current iteration and k denotes previous iteration. The parameter Δ is a constant from the interval of $(0.1,0.3)$ or can be iteratively determined (sub-optimization task) for each iteration k using the line search method (SD-LS). In Equation (9) F^k denotes the value of the objective function in the k-th iteration, whereas $F_{,\alpha}$ is the gradient of the objective function. This gradient can be computed using the following relation:

$$F_{,\alpha}=\frac{\partial F}{\partial \mu_\alpha}=\frac{\partial F}{\partial f_i}\frac{\partial f_i}{\partial \overset{0}{\kappa}_\gamma}\frac{\partial \overset{0}{\kappa}_\gamma}{\partial \mu_\alpha} \qquad \text{or} \qquad F_{,\alpha}=\frac{\partial F}{\partial \mu_\alpha}=\frac{\partial F}{\partial f_i}\frac{\partial f_i}{\partial \overset{0}{\varepsilon}_\gamma}\frac{\partial \overset{0}{\varepsilon}_\gamma}{\partial \mu_\alpha}. \tag{10}$$

The termination of the optimization process follows when decrease of the objective function reaches either the pre-determined level (e.g 10^{-5}) or the number of iterations.

2. NUMERICAL EXAMPLES

The numerical tests were preformed using the two-dimensional frame structure shown in Figure 2(a). All its steel elements with length of 51cm have rectangular-shaped cross sections: $80\,\text{mm}\times 8\,\text{mm}$, density $\rho=7850\,\frac{\text{kg}}{\text{m}^3}$ and Young's modulus $E=210\,\text{GPa}$. Two load scenarios were considered: the bending moment was applied either to node 5 or node 7 with the Gauss-like function series in the time domain as presented in Figure 2(b).

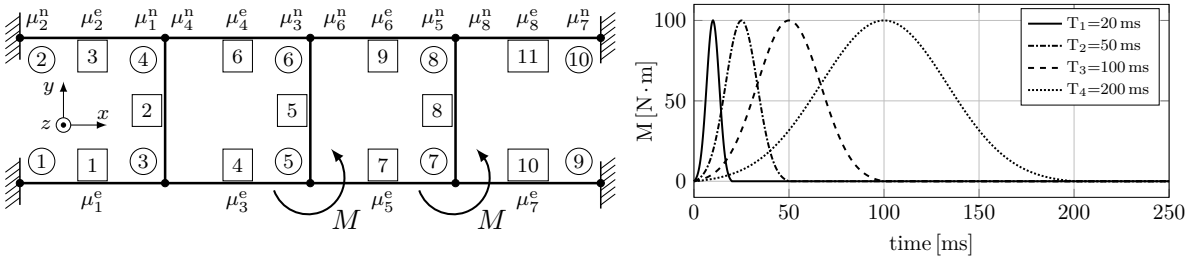

(a) (b)

Figure 2 : (a) The scheme of the tested frame structure. (b) The load test functions applied either to node 5 or 7.

The components of the nodal modification vector μ_α^n ($\alpha=1,2..8$) are marked in Figure 2(a). According to the notation, μ_1^n denotes the dimensionless value of the nodal stiffness connection for element 3 in node 4. All these components are unit at first step in the optimization procedure and are limited to be in the range $\langle 0,1\rangle$ in next iterations. The vector of the element stiffness modification μ_α^e has also 8 components which are numbered as shown in Figure 2(a).

At first, the dynamic analysis of the original structure was performed using the Newmark's integration method with the number of $n=501$ time steps ($\Delta t=4\cdot 10^{-4}\,\text{s}$). The accelerations at node

8 along the x and y axis were selected as the structural response for defining the objective function (cf. Equation (8)). For determining the virtual distortions the corresponding influence matrices $B_{\alpha\beta}(t)$ (dimensions: $8 \times 8 \times 501$), $D_{\alpha\beta}(t)$ ($24 \times 24 \times 501$) and for updating the accelerations the generalized influence matrices $\hat{B}_{\alpha\beta}(t)$ ($2 \times 8 \times 501$), $\hat{D}_{\alpha\beta}(t)$ ($2 \times 24 \times 501$) were pre-computed.

2.1 Modification of the nodal stiffness connections

For the assumed modifications $\mu_3^{\mathrm{n}} = 0.5$ and $\mu_4^{\mathrm{n}} = 0.5$ at nodes 4 and 6 respectively, the accelerations at node 8 were computed for the two load scenarios: at node 5 (scenario I) and at node 7 (scenario II). For each load scenario, four test time-functions as illustrated in Figure 2(b) were applied. Altogether, there were 8 optimisation problems to be solved. The solutions were obtained using the steepest descent method (SD) twice: with and without line-search. The optimization results obtained for the load scenario I are presented in Figure 3(a). In the logarithmically scaled vertical axis, normalized values of the objective function during iterations are shown. The current value is referred to the value computed at the first iteration. In Figure 3(c) the identified nodal stiffness parameters μ_α^{n} are illustrated. Generally, the obtained solution is not precisely, however correctly indicates the localization of nodal modifications (except for the test function T_2). On the contrary, for the load scenario II the localization of the nodal modifications were not indicated satisfactorily.

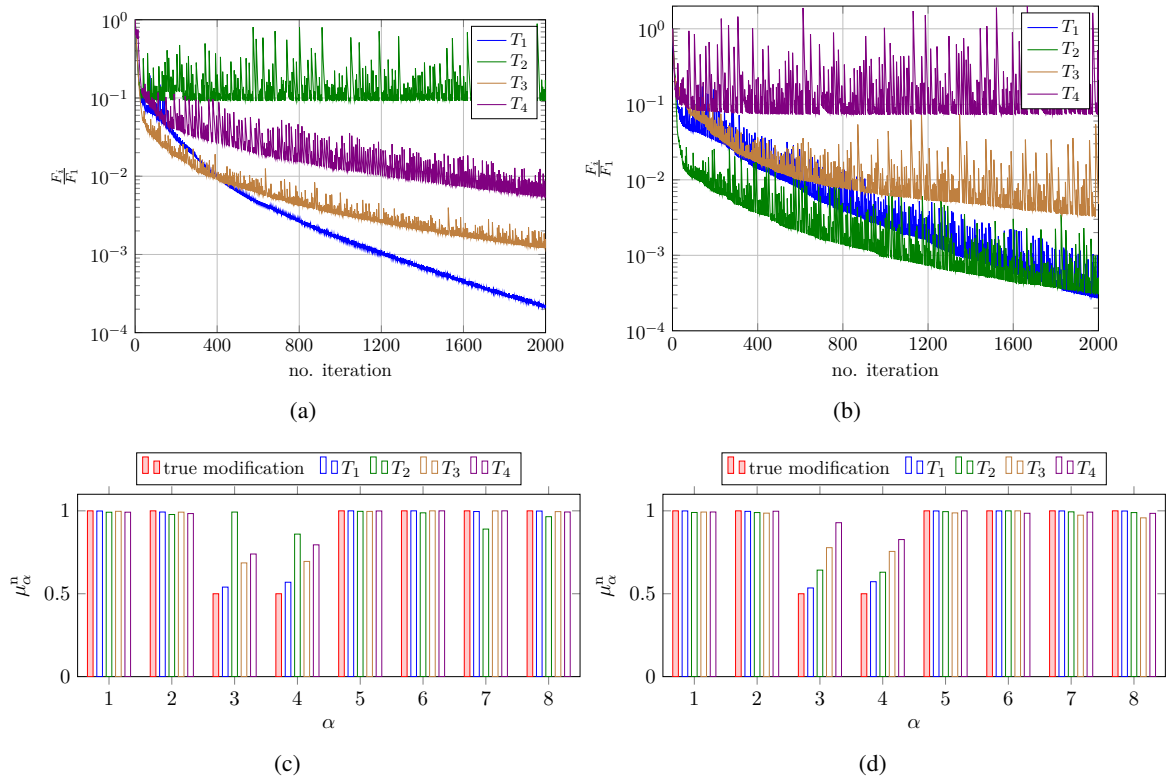

Figure 3 : Optimization results obtained for the load scenario I (node 5): (a) decreasing of the objective function using SD method and (b) SD-LS method, (c) the identified the nodal stiffness parameters using SD method and (d) SD-LS method.

The computations were repeated using an additional structural response – accelerations along y in node 6. For this case the normalized values of the objective functions and the identified parameters μ_α^{n} are presented in Figure 3(b) and Figure 3(d), respectively. From those charts one can see increase of

the precision of the solutions. For assessment of the solution accuracy let us define an error function e:

$$e = \sum_{\alpha} |\hat{\mu}_\alpha - \bar{\mu}_\alpha|, \tag{11}$$

where $\hat{\mu}_\alpha$ the real modification parameter and $\bar{\mu}_\alpha$ identified one. A set of the values e for the considered optimization problems contains Table 1.

2.2 Modification of the stiffness of elements

Similarly to the previous subsection, for the stiffness modifications (Young's modulus) two elements were selected: element no. 4 (with $\mu^{\mathrm{e}}_3 = 0.5$) and element no. 9 (with $\mu^{\mathrm{e}}_6 = 0.5$). The dynamic responses (assumed two sensors) were recalculated for modified structure using the discussed testing loads. Analogously to the previous optimization tasks, the solutions were computed using SD and SD-LS methods using 500 and 125 iterations, respectively. The results obtained using SD method for the load scenarios I and II are shown in Figure 4.

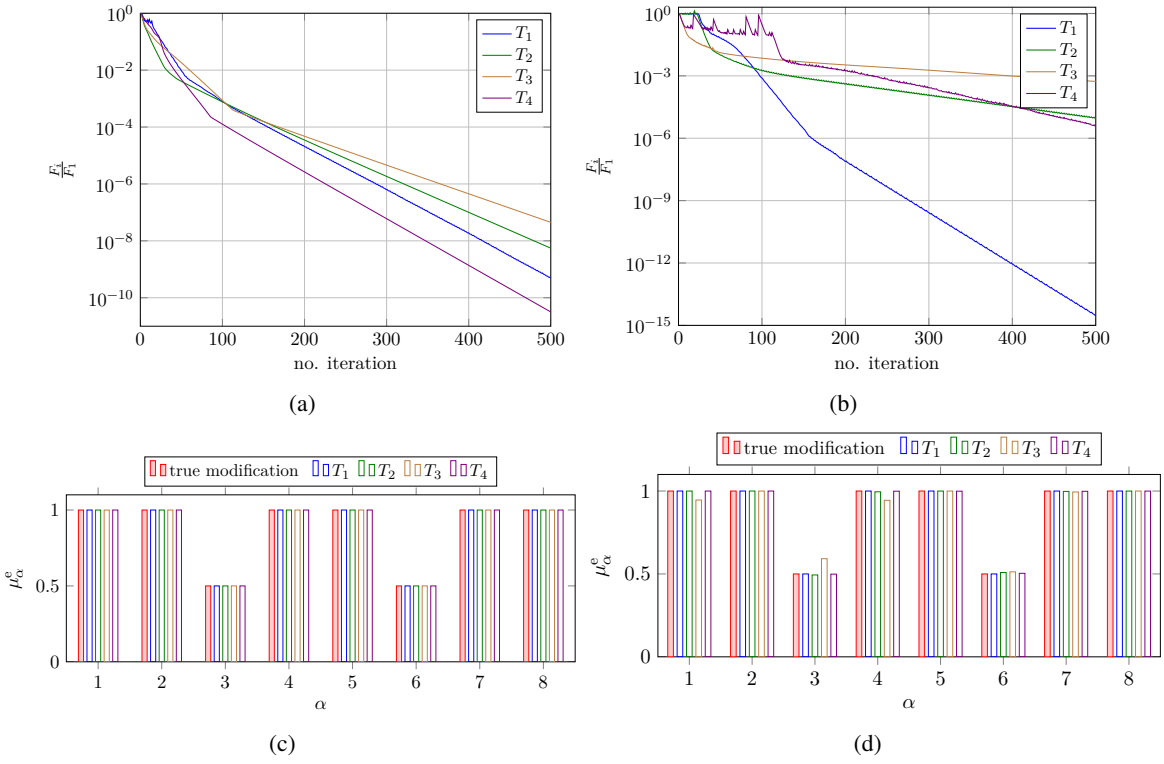

Figure 4 : Optimization results obtained for the load scenario I (node 5): (a) decreasing of the objective function using SD method and (b) SD-LS method, (c) the identified the element stiffness parameters using SD method and (d) SD-LS method.

In case of identification of element stiffness parameters μ^{e}_α, the required number of iterations is significantly less. Simultaneously, the resulting solution is very close to the real modifications, especially for load scenario I (cf. Table 1).

In Figure 5 the computed acceleration in node 8 for the load scenario I (T_1) is shown. The red line corresponds to the original structure, whereas the blue and green ones are obtained for the structural modification parameters $\hat{\mu}^{\mathrm{n}}_\alpha$ and $\hat{\mu}^{\mathrm{e}}_\alpha$, respectively. All the responses are clearly different. During the optimization process, the modification parameters $\bar{\mu}^{\mathrm{n}}_\alpha$ were identified such that the modelled response (dashed black curve) covers the response of the modified structure.

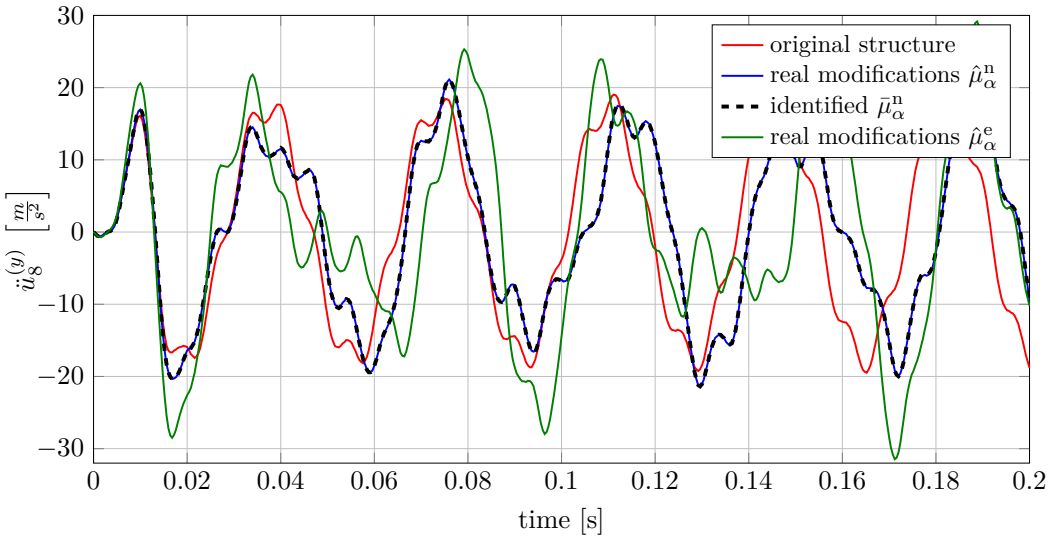

Figure 5 : A comparison of the acceleration obtained in node 8 along y axis under the load scenario I with the test function T_1.

3. SUMMARY

Table 1 contains the values of the error function according to Equation (11) computed for the all discussed optimized stiffness parameters. Generally, the smaller values are obtained for the impulses with shorter time duration, but on the other hand it does not guarantee the rapid convergence of solutions. The resulting values e calculated for the nodal stiffness parameters are higher than for the element stiffness parameters, however the obtained modelled responses reflect the responses of the modified structure very precisely (cf. Figure 5).

Table 1 : Values of the error function computed using Equation (11) and the identified stiffness parameters.

Load scenario	**Value of the error function**					
	Identification of the nodal connections				**Identification of the stiffness of elements**	
	SD	**SD-LS**	**SD***	**SD-LS***	**SD**	**SD-LS**
I (T_1)	0.12	0.69	0.11	0.15	$4.3 \cdot 10^{-5}$	$1.2 \cdot 10^{-2}$
I (T_2)	1.04	0.77	0.31	0.60	$1.7 \cdot 10^{-4}$	$1.1 \cdot 10^{-3}$
I (T_3)	0.40	0.76	0.63	0.87	$4.7 \cdot 10^{-4}$	$2.1 \cdot 10^{-3}$
I (T_4)	0.57	0.84	0.80	0.71	$1.4 \cdot 10^{-5}$	$1.1 \cdot 10^{-3}$
II (T_1)	1.62	1.43	1.37	1.31	$< 1 \cdot 10^{-6}$	$3.2 \cdot 10^{-4}$
II (T_2)	0.11	0.68	0.12	0.64	$2.2 \cdot 10^{-2}$	1.33
II (T_3)	1.21	0.83	1.10	0.87	0.22	0.79
II (T_4)	1.56	1.50	0.52	1.11	$8.8 \cdot 10^{-3}$	$6.5 \cdot 10^{-2}$

*computations performed with additional sensor

This study explores the modelling and identification of semi-rigid nodal connections and stiffness of elements in 2D frame structures based on Bernoulli's beam theory using finite element method without modification of a local element stiffness matrix. Instead, for such modifications the virtual

distortions field is imposed on the original structure. The basis for calculating of the updated dynamic responses for the modified structure are the influence matrices. This approach allows for computation of analytical gradients of the virtual distortions with respect to the vector of modification parameters. Therefore, it is useful for solving the gradient-based optimization problems aimed at determination of the parameters for the nodal semi-rigid connections. The objective function is expressed in terms of responses obtained for the original and modified structure under the same load. In this paper, a numerical example of identification of the nodal stiffness modification for the simple frame structure was successfully performed.

ACKNOWLEDGEMENT

The support of Structural Funds in the Operational Programme Innovative Economy (IE OP) financed from the European Regional Development Fund Projects Modern Material Technologies in Aerospace Industry (POIG.0101.02-00-015/08) and the FP7 EU project Smart-Nest (PIAPP-GA-2011-28499) is gratefully acknowledged.

REFERENCES

[1] M.A. Akgun, J.H. Garcelon, R.T. Haftka, Fast Exact Linear and Non-linear Structural Reanalysis and the Sherman-Morrison-Woodbury Formulas, International Journal for Numerical Methods in Engineering, 2001, vol. 50, pp. 1587-1606.

[2] P. Kolakowski, A. Swiercz, K. Sekula, A Concept of Long-Term Monitoring of a Railway Truss Bridge Excited by Trains, Proceedings of the 4th European Workshop on Structural Health Monitoring, 2008, pp. 175-182, Cracow, Poland.

[3] A. Swiercz, P. Kolakowski, J. Holnicki-Szulc, Identification of damage using low frequency harmonics in trusses and beams, Proceedings of ISMA2006: International Conference on Noise and Vibration Engineering, 2006, pp. 2137-2144, Leuven, Belgium.

[4] A. Swiercz, P. Kolakowski, J. Holnicki-Szulc, Damage identification in skeletal structures using the virtual distortion method in frequency domain Mechanical Systems and Signal Processing, 2008, vol. 22 no. 8, pp. 1826-1839.

[5] P. Kolakowski, J. Holnicki-Szulc, Optimal Remodelling of Truss Structures – Simulation by Virtual Distortions, Computer Assisted Mechanics and Engineering Sciences, 1997, no. 4, pp. 257-281.

[6] P. Kolakowski, M. Wiklo, J. Holnicki-Szulc, The virtual distortion method – a versatile reanalysis tool for structures and systems Structural and Multidisciplinary Optimization, 2008, vol. 36, no. 3, pp. 217-234.

[7] A. Swiercz, P. Kolakowski, J. Holnicki-Szulc, Monitoring of progressive collapse of skeletal structures, 9th International Conference on Damage Assessment of Structures (DAMAS 2011), Book Series: Journal of Physics Conference Series, 2011, vol. 305, doi: 10.1088/1742-6596/305/1/012133, 012133, Oxford, England.

[8] M. Wiklo, J. Holnicki-Szulc, Optimal design of adaptive structures: Part I. Remodeling for impact reception, Structural and Multidisciplinary Optimization, 2009, vol. 37, no. 3, pp. 305-318.

[9] M. Wiklo, J. Holnicki-Szulc, Optimal design of adaptive structures: Part II. Adaptation to impact loads, Structural and Multidisciplinary Optimization, 2009, vol. 37, no. 4, pp. 351-366.

[10] J. Holnicki-Szulc, P. Kolakowski, N. Nasher, Leakage Detection in Water Networks, Journal of Intelligent Material Systems and Structures, 2005, vol. 16, no. 3, pp. 207-219.

[11] A. Orlowska, P. Kolakowski, J. Holnicki-Szulc, Modelling and Identification of Delamination in Double-Layer Beams by the Virtual Distortion Method, Computers and Structures, 2008, vol. 86, issue 23-24, pp. 2203-2214.

[12] M. Kokot, J. Holnicki-Szulc, Defect Identification in Electrical Circuits via the Virtual Distortion Method. Part 1: Steady-state Case, Journal of Intelligent Material Systems and Structures, 2009, vol. 20, no. 12, pp. 1465-1473.

[13] A. Swiercz, P. Kołakowski, J. Holnicki-Szulc, D. Olkowicz, Identification of semi-rigid joints in frame structures, 6th ECCOMAS Conference on Smart Structures and Materials, 2013.

[14] J. Holnicki-Szulc (Ed.), Smart Technologies for Safety Engineering, Wiley, 2008.